http://dx.doi.org/10.5755/j01.eee.19.4.1846 ELEKTRONIKA IR ELEKTROTECHNIKA, ISSN 1392-1215, VOL. 19, NO. 4, 2013

# Measurement of Air Bubbles Concentration in the Water by Means of Digital Image Processing

A. Vaideliene[1,2], P. Tervydis[3]
[1]Department of Physics, Kaunas University of Technology,
Studentu St. 50, LT-51368 Kaunas, Lithuania,
[2]Lithuanian Energy Institute,
Breslaujos St. 3, LT-44403 Kaunas, Lithuania, phone: +370 37 401966
[3]Department of Telecommunications, Kaunas University of Technology,
Studentu St. 50, LT-51368 Kaunas, Lithuania, phone: +370 37 300516
avaidel@mail.lei.lt

***Abstract*—While fluids are falling into air-water boundaries, the entrainment of air occurs below this surface. Water aeration takes place and it`s range is defined by the concentration of formed bubbles. This paper presents a method to measure the concentration of air bubbles using digital image processing. For analysis of digital camera images library Python 2.7 was used.**

***Index Terms*—Optical methods, air bubbles concentration, digital image processing.**

## I. INTRODUCTION

The interaction between falling water and the air leads to gas entrainment into water and strong air-water mixing. Hydraulic, mechanical, chemical and nuclear power engineering encounters the phenomenon of air bubble entrainment. In nature, air bubble entrainment into water takes place at spillways of weirs, at river overfalls, in mountain streams and in breaking waves on the ocean surface.

During the last decade many experimental and theoretical investigations in laminar as well in turbulent liquid flows were accomplished. The results show that the concentration of air bubbles in the water greatly depends on the geometrical configuration of water jet, and boundary conditions of water mixing [1-3]. It was also determined that the amount of air bubbles, and their distribution in the water depends on the height of the jet, and the velocity of the jet at the moment it hits the water's surface [4].

A new focus is digital simulation of this transfer mechanism of air bubbles and water droplets in turbulent flow which allows predicting of this process trend. Squires and Eaton were the first who investigated digital simulation of particles transfer in homogeneous isotropic stationary systems [5]. Fuster and Colonius further developed digital simulation of processes taking place in turbulent flows, using methods of mathematical optimization [6].

With an increasing number of experimental investigations of water droplet and air bubble mixtures, accuracy of measurement and reliability of these results become more important. Many methods were used for the measurement of relative concentration of water droplets and air bubbles in the water air mixture. The prevalent method now used is the measurement of the conductivity of the water-air mixture. This method is not accurate, though, since it does not evaluate the concentration in the separate layers of the mixture.

This paper presents a new method of measuring water droplet and air bubble concentrations in all layers of mixture based on digital image processing [7].

Manuscript received June 8, 2012; accepted November 12, 2012.

## II. THE THEORETICAL AIR ENTRAINMENT MODEL

Water flow, falling into a water reservoir's surface, deforms the water surface and creates a turbulent flow that causes air entrainment into the deeper layers of water. Air bubble entrainment in to the water occurs when turbulent shear stress exceeds the surface tension and buoyancy forces. In this case turbulent energy cracks the water-air boundary surface and forms a small turbulent structure with eddies in the deeper water layers. Experimental results of many independent researchers show that a water jet also creates surface undulation, that on its own part stimulate air entrainment into water. Thus air entrainment into water depends on jet parameters as well as on water-air boundary layer conditions.

The condition of air entrainment can be expressed as follows [8]

$$\left|\rho_v \cdot v_i \cdot v_j\right| > \sigma \frac{\pi \cdot (r_1 + r_2)}{A}, \quad (1)$$

where $\rho_v$ – density of water, $v$ – fluctuation of turbulent velocity, $\sigma$ – water surface tension, $\pi(r_1+r_2)$ – perimeter along surface tension, $A$ – area of surface.

The eq. (1) determines initial condition of air bubble entrainment into water.

The concentration of air bubbles entrained into the water depends on nozzle parameters such as a diameter $d_0$, distance between jet and water surface $L$, initial speed of jet $v_0$, and $v_1$ is the jet speed at the moment it hits the water surface (Fig. 1).

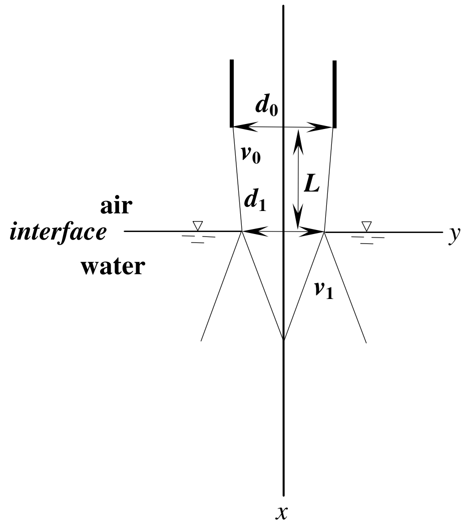


Fig. 1. Scheme of air entrainment into water with vertical jet.

H. Chanson his experimental results described with this empirical equation [10]

$$C_{air} = \frac{q_{air}}{q_w} \frac{1}{4D_m \frac{(x-L)}{Y_{C\max}}} \exp\left( -\frac{1}{4D_m} \frac{\left(\frac{y}{Y_{C\max}}\right)^2 + 1}{\frac{(x-L)}{Y_{C\max}}} \right) \times$$

$$\times I_0 \left( \frac{1}{2D_m} \frac{\left(\frac{y}{Y_{C\max}}\right)}{\frac{(x-L)}{Y_{C\max}}} \right), \quad (2)$$

where $q_w$ is the water flow rate, $q_{air}$ is the air flux, $x$ is the longitudinal coordinate, $D_m$ is dimensionless air bubble diffusion coefficient, $I_0$ is the first kind modified Bessel function of order zero, $L$ is the distance between jet nozzle and water surface, $Y_{Cmax}$ is the distance from the jet centerline where the air concentration is maximum.

Sande and Smith calculate the entrainment air flux by low velocity (2–5 m/s) turbulent water jets plunging into quiescent pool of water using the formula below [9]

$$q_{air} = 0.021 \frac{d_1^3 v_1^2 L^{\frac{1}{3}}}{\sin\alpha}, \quad (3)$$

where $\alpha$ is the jet impingement angle.

The maximum depth of air entrainment in to water can be calculated as follow [8]

$$h = \frac{2.1 v_1^{0.775} d_0^{0.625}}{L^{0,094}}. \quad (4)$$

## III. The Method of Air Bubble Measurement

Many researchers determine the concentration of air bubbles entrained into water by means of conductivity measurement [10-12]. With this work we present a new method for air bubble concentration measurement, which is based on digital analysis of air bubble images fixed with digital photo camera (Fig. 2). For the experiment a 0.2 m deep glass vessel and vertical nozzle were used. Images from a digital photo camera were analysed using Python 2.7 with Python Imaging Library (PIL).

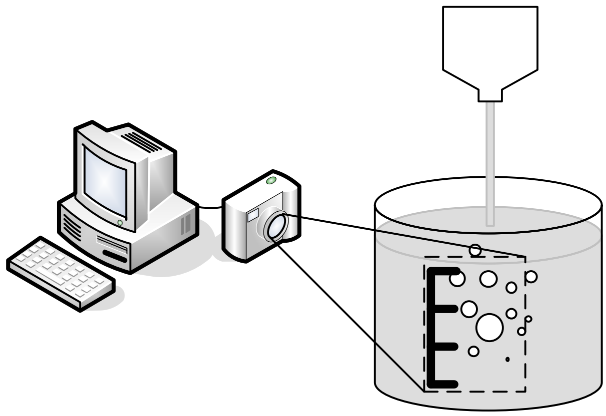

Fig. 2. Scheme of experiment equipment.

The main idea of our method can be explained using the Fig. 3. The left side of the image is the photo of water with air bubbles, the right side – the modified image, where air bubbles are presented as black spots. It is clear from the visual analysis of the left image, that the air bubbles are much brighter than the background. It can be used to evaluate the air bubble concentration in the water.

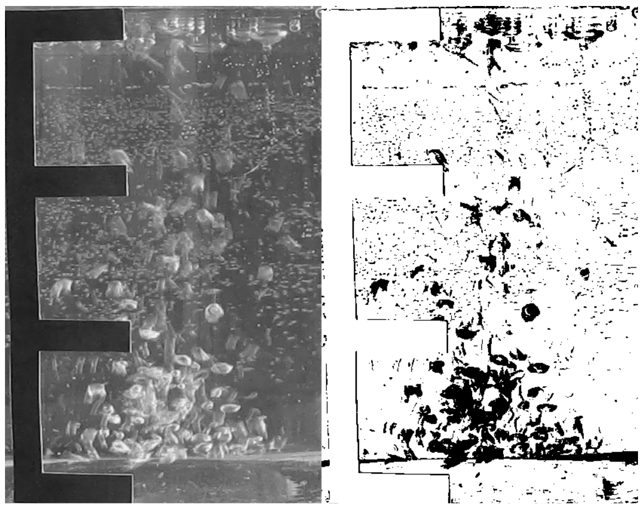

(a) (b)

Fig. 3. The example of image analysis: (a) – the photo with air bubbles in the water, (b) – the image with white background and black spots instead of air bubbles.

For that purpose the photo is converted to the greyscale image. The greyscale image is composed exclusively of shades of grey, varying from black at the weakest intensity to white at the strongest. Binary representations of greyscale assume that 0 is black and the maximum value 255 is white (Fig. 4). The image on the right side of the Fig. 3 is achieved by replacing pixel greyscale values according to the scheme that is presented in Fig. 4. If a pixel value is > 145, then the pixel value is set to 0, otherwise it is set to 255.

Thus the air bubble concentration can be calculated by

$$C_{air} = \frac{N_b}{N_w + N_b}, \quad (5)$$

where $C_{air}$ –air bubble concentration $N_b$ – number of black pixels, $N_w$ – number of white pixels.

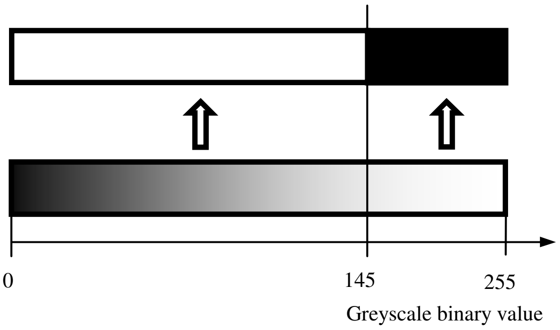


Fig. 4. Pixel value replacement scheme.

The presented image analysis example was made by the following Python code:

```
from PIL import Image
image_file = "experiment.png"
image1 = Image.open(image_file).convert('L')
image2 = Image.open(image_file).convert('L')
pix1 = image1.load()
pix2 = image2.load()
box = image1.getbbox()
xmax = box[-2]
ymax = box[-1]
Nb = 0.0
Nw = 0.0
for x in range(xmax):
  for y in range(ymax):
    val = pix1[x,y]
    if val > 145:
      pix2[x,y] = 0
      Nb = Nb+1
    else:
      pix2[x,y] = 255
      Nw = Nw+1
Cair = Nb/(Nb+Nw)
print "Air bubble concentration - Cair=",Cair
blank_image = Image.new("L",(2*xmax, ymax))
blank_image.paste(image1, (0,0))
blank_image.paste(image2, (xmax,0))
blank_image.save("result.png")
```

## IV. The Air Bubble Entrainment Experimental Results

In this section we present the experimental results, which were achieved using our proposed air bubble concentration analysis method.

The method was improved to evaluate how the air bubble concentration is dispersed in water. It should be possible to evaluate the depth of entrained air bubbles and their distribution based on deepness the $C_{air}$ value for every line of pixels must be known. Knowing how many pixels contains 1 cm, the air bubbles concentration in the particular depth can be exactly calculated. How many pixels contains 1 cm can be easily determined from scale given in Fig. 4.

With determined $C_{air}$ values for every pixels column air bubbles distribution in width can be evaluated.

Fig. 5 represents case, when there is no falling water and no air bubbles entrainment in to the water. The dependencies of air bubbles concentration on depths $C_{air}(h)$ are shown at right side of the picture, and on the width $C_{air}(w)$ – at the bottom. Despite of it, that there is no air bubbles entrainment, on the walls of vessel the air bubbles can be seen. The maximum value of $C_{air}(h)$ dependence is at the depth of 14.5 cm. Glass vessel's edge is seen at this depth. The maximum value of $C_{air}(w)$ dependence is, when $w = 1$ cm. It makes white edge of paper scale glued to the glass.

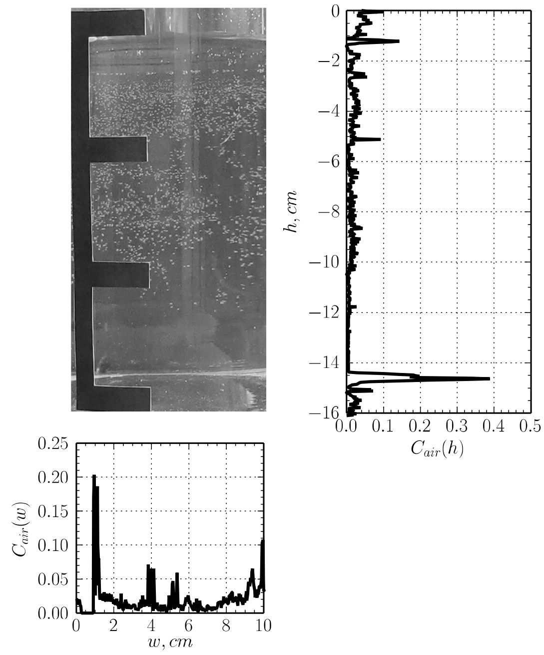


Fig. 5. Experiment results with no air entrainment.

Fig. 6 depicts image with low intensity air bubbles entrainment and $C_{air}(h)$ and $C_{air}(w)$ dependencies.

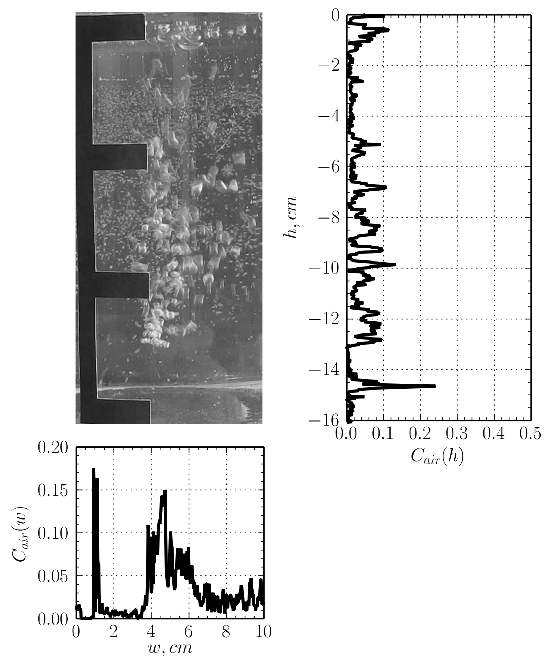


Fig. 6. Experiment results with low intensity air entrainment.

Fig. 7 depicts image with high intensity air bubbles entrainment and $C_{air}(h)$ and $C_{air}(w)$ dependencies.

The results of experiment apparently show that proposed method can be used for evaluation of concentration of air bubbles entrained in to water.

The received results could be influenced by black scale glued to the glass wall of the vessel. This scale shields part of the bubbles and white its edge, bottom of vessel and reflections can distort proper values of air bubbles concentration.

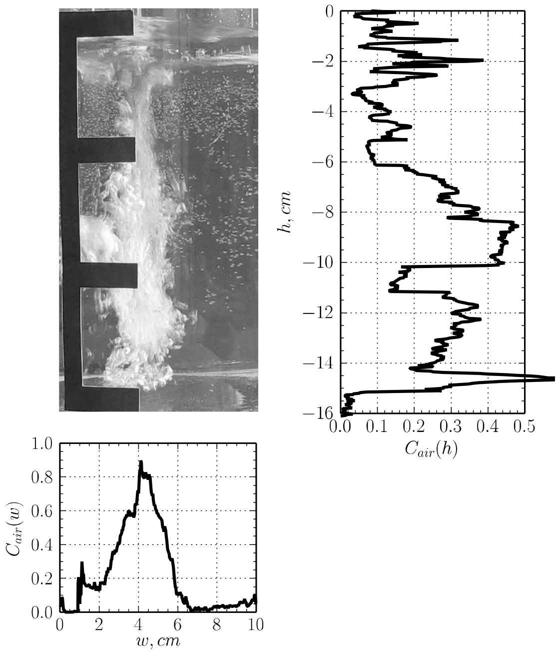


Fig. 7. High intensity air entrainment experimental results.

## V. CONCLUSIONS

1. Concentration of air bubbles entrained in to water can be determined by means of digital image processing (DIP).

2. DIP allows calculating of air bubbles concentration as the function of depth, as well as a function of width.

3. Experimental received distribution of air bubbles concentration coincides with theoretically obtained distribution.

## REFERENCES

[1] S. P. Malinowski, “Turbulent mixing of cloud with the environment: Two – phase evaporating flow. Numerical simulations, laboratory experiments and field measurements”, *J. theoretical and applied mechanics,* Warsaw, no. 45, pp. 587–601, 2007.

[2] E. Aulisa, S. Manservisi, R. Scardovelli, S. Zaleski, „Interface reconstruction with least-squares fit and split advection in three-dimensional Cartesian geometry“, *J. of Computational Physics,* vol. 225, pp. 2301–2319, 2007. [Online]. Available: http://dx.doi.org/10.1016/j.jcp.2007.03.015

[3] A. Vaidelienė, V. Vaidelys, “Air bubbles and water droplets entrainment and removal in turbulent water flows”, *Mechanika*, vol. 18, no. 1, pp. 56–62, 2012. [Online]. Available: http://dx.doi.org/10.5755/j01.mech.18.1.1282

[4] P. K. Panday, “Two-dimensional turbulent film condensation of vapours flowing inside a vertical tube and between parallel plates: a numerical approach”, *Int. J. of Refrigeration,* no. 26, pp. 492–503, 2003.

[5] K. D. Squires, J. K. Eaton, „Preferential concentration of particles by turbulence‘, *Phys. Fluids*, no. A 3, 1991.

[6] D. Fuster, T. Colonius, „Modeling bubble clusters in compressible liquids“, *J. of Fluid Mechanics,* vol. 688, pp. 352–389, 2011. [Online]. Available: http://dx.doi.org/10.1017/jfm.2011.380

[7] J. Valantinas, D. Kančelkis, “Speeding-up Image Encoding Times in the SPIHT Algoritm” *Information Technology and Control,* vol. 40, no. 1, pp. 7–12, 2011. [Online]. Available: http://dx.doi.org/10.5755/j01.itc.40.1.187

[8] H. Chanson, *Fluid Mechanics of Environmental Interfaces*, Taylor & Francis, 2008, p. 196.

[9] E. Sande, J. M. Smith, „Mass transfer from plunging water jets“, *Chemical Eng. J.,* vol. 10, pp. 225–233, 1975.

[10] L. Toombes , H. Chanson, “Interfacial aeration and bubble count rate distributions in a supercritical flow past a backward-facing step”, *Int. J.l of Multiphase Flow*, no. 34, pp. 427–436, 2008. [Online]. Available: http://dx.doi.org/10.1016/j.ijmultiphaseflow.2008.01.005

[11] H. Chanson, T. Brattberg, “Experimental study of the air-water shear flow in a hydraulic jump”, *Int. J. of Multiphase Flow,* no. 26, pp. 583–607, 2000. [Online]. Available: http://dx.doi.org/10.1016/S0301-9322(99)00016-6

[12] F. Murzyn, H. Chanson, “Free-surface fluctuations in hydraulic jumps: Experimental observations”, *Experimental Thermal and Fluid Science,* vol. 33, no. 7, pp. 1055–1064, 2009. [Online]. Available: http://dx.doi.org/10.1016/j.expthermflusci.2009.06.003